Colloid & Polymer Science Colloid Polym Sci 270:370–376 (1992)

Dynamic surface tension of micellar solutions studied by the maximum bubble pressure method. 1. Experiment

Tz. H. Iliev*,†) and C. D. Dushkin*)

*) Laboratory of Thermodynamics and Physico-chemical Hydrodynamics, Faculty of Chemistry, University of Sofia, Sofia, Bulgaria
†) Institute of Geology, Bulgarian Academy of Sciences, Sofia, Bulgaria

Abstract: The effect of the micelles on the dynamic surface tension of micellar surfactant solutions is studied experimentally by means of the maximum bubble pressure method. Different frequencies of bubbling ranging approximately between 1 and 30 s^{-1} are applied. The time dependence of the surface tension is calculated using a dead time correction. Water solutions of two types of surfactants with different concentrations are investigated: sodium dodecyl sulfate and nonylphenol polyglycol ether. The surface tension relaxes more quickly in the presence of micelles. The characteristic times of relaxation of the surface tension seem to be in the millisecond range. The time constants observed experimentally are explained in terms of the theory of surfactant diffusion affected by micellization kinetics.

Key words: Dynamic surface tension; micellar surfactant solutions; maximum bubble pressure method

Introduction

Dynamic surface tension, $\sigma(t)$, is a physical quantity associated with a deformation of fluid interfaces (air/water or oil/water), when surface active material is present in the liquids. In this case the surface tension may be a peculiar function of time t. It depends on the way the surfactant is transported from the bulk of solution to the interface, where it adsorbs. Therefore, by measuring the dynamic surface tension, one can study the mass transfer processes, which are of importance for the stability of a number of disperse systems such as foams and emulsions. If the surfactant concentration exceeds the critical micelle concentration (CMC), micelles are formed in the solution. These aggregates appear as additional sources of material which can appreciably affect the mass transfer and, hence, the dynamic surface tension.

An appropriate tool for measuring the dynamic surface tension is the maximum bubble pressure method (MBP-method). In this method air bubbles are blown away by a capillary immersed in the surfactant solution. The bubbling frequency is ν. By varying ν the age of the bubble surface changes, thus making different time intervals t accessible.

Many authors have used the MBP-method to study the dynamic surface tension of a variety of surfactant solutions (see, e.g., [1–5]). Here, we will concentrate on the studies with sodium dodecyl sulfate (SDS), because SDS is also used in our experiments. These are the papers of Kloubek [6], Feinerman [7–9], Miller and Meyer [10], Woolfrey et al. [11], Garrett and Ward [12]. A typical relaxation of the surface tension σ is found. Initially (at zero time), σ is close to the value of the surface tension of pure water. When time increases (frequency of bubbling ν decreases), σ lowers, tending to its equilibrium value. The equilibrium surface tension $\bar{\sigma}$ can be reached after infinite time. If the surfactant concentration, $\bar{c}$, increases, the relaxation of the surface tension becomes faster. At fixed

t the curve $\sigma(\bar{c})$ undergoes change around CMC, which is less pronounced than the respective change in the equilibrium isotherm $\bar{\sigma}(\bar{c})$ [11].

The literature data for SDS exhibit the main features of the dynamic surface tension of micellar solutions. However, they are not so useful for quantitative considerations above CMC by means of a theoretical model. Therefore, one needs accurate data for the dynamic surface tension of SDS solutions, which can be used to compute the parameters of the micellization kinetics.

The other surfactant used in our investigations is Veranol H10 (nonylphenol polyglycol ether, 10 mol ethyleneoxide groups). Veranol H10 is a nonionic commercial surfactant. Only few data for this surfactant are available in the literature [13] (see below).

The purpose of our study is to utilize the MBP-method as a tool for studying the kinetics of micellization in water surfactant solutions. In this paper, we present the experimental results for the dynamic surface tension of micellar solutions of SDS and Veranol H10, obtained by us. In subsequent papers [14, 15] we will propose a diffusion theory of the dynamic surface tension of micellar solutions, which allows the time constants of diffusion and micellization to be evaluated from the experimental data.

Materials

SDS is produced by Touzart & Matignon (pur.). Veranol H10 is supplied by Verila Co. Both surfactants are used without further purification. The surfactant solutions were prepared with distilled water. The measurements were carried out no more than 2 days after preparation of the solutions. The room temperature was maintained at $25 \pm 1\,^{\circ}\mathrm{C}$.

Experimental setup

In Fig. 1 is depicted the MBP experimental setup constructed by us. It is similar to that used very recently by Garrett and Ward [12] for studying the dynamic surface tension of SDS solutions. The surfactant solution (around 90 ml) is filled in a cylindrical glass cell with an internal diameter 3.5 cm. The bubbles are formed at the tip of a capillary with an internal radius $R_c = 7.5 \times 10^{-3}$ cm. The capillary is immersed in the surfactant solution. The pressure difference $\Delta P = P_a - P_w$,

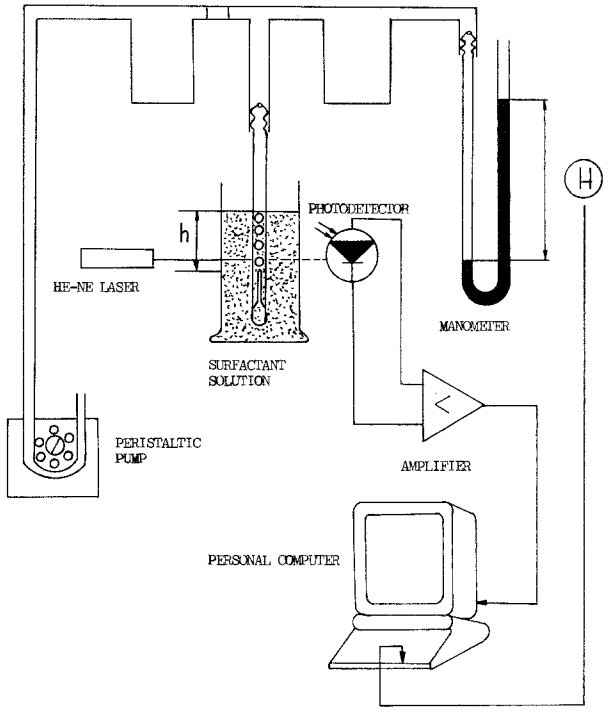

Fig. 1. Experimental setup for measuring the dynamic surface tension by the MBP-method

produced by a peristaltic pump, is measured by a water manometer (P_a – pressure in the air phase, P_w – pressure in the water phase). The maximum pressure, ΔP_{max}, is calculated by the formula

$$\Delta P_{max} = \Delta\rho g(H - h)\,. \tag{1}$$

Here, $\Delta\rho = \rho_w - \rho_a$ is the density difference (ρ_w – water density, ρ_a – air density); H is the difference between the levels of the water in the two sections of the monometer; h is the difference between the tip of the capillary and the air/solution surface in the cell. Both quantities H and h are measured precisely by a cathetus-meter.

The frequency of bubbling ν is registered by means of an electro-optical system. It consists of 2 mW He-Ne laser, photodiode, amplifier and personal computer. After the bubble leaves the tip of the capillary it overshadows the laser beam, which pierces the whole cylinder and the surfactant solution inside. The alternating interruption of the beam is detected by the photodiode; after which the signal is amplified and processed by the computer. In this way the frequency ν is determined with an accuracy of $10^{-2}\,\mathrm{s}^{-1}$.

Calculation of the surface tension

The dynamic surface tension $\sigma(t)$ corresponds to the maximum pressure ΔP_{max} (see below). At that time the bubble is approximately a hemisphere with a radius R_c. The force

balance across the bubble surface gives [16] (see Appendix)

$$\sigma = \frac{1}{2} R_c \Delta P_{max} \left(1 - \frac{2\Delta\rho g R_c}{3\Delta P_{max}} \right), \quad (2)$$

where the second term in parentheses accounts for the gravitation. Let us introduce the Eötvös number Eo

$$Eo = \Delta\rho g R_c^2 / 2\sigma .$$

In this way, Eq. (2) becomes

$$y = 1 - (2/3) Eo(y) y , \quad (3)$$

where, in view of Eq. (1):

$$y = 2\sigma / R_c \Delta\rho g (H - h) .$$

Equation (3) can easily be solved by means of the method of asymptotic expansions [17]. The formal solution of Eq. (3) reads

$$y = 1 + \sum_{k=1}^{\infty} (-2/3)^k Eo^k(y) . \quad (4)$$

The value of σ can be obtained with an appropriate accuracy from Eq. (4) by an iterative procedure.

Let us compare Eq. (4), written in the form

$$y = 1.0 - 0.6667 Eo + 0.4444 Eo^2 \quad (5)$$

with other equations, available in the literature. The equation of Bendure [3] reads

$$y = 0.9995 + 0.0136 Eo^{1/2} - 0.1113 Eo^{3/2} + 0.5647 Eo^2 , \quad (6)$$

while the equation of Johnson and Lane [18] is

$$y = 1.0 - 0.6622 Eo - 0.0603 Eo^{3/2} + 0.5631 Eo^2 . \quad (7)$$

Equations (6) and (7) are obtained numerically by interpolation of the tables of Sugden [19]. The exact analytical solution of the problem, Eq. (5), explains why the contribution of the odd powers of $Eo^{1/2}$ in Eqs. (6) and (7) is negligible. Another solution of the Laplace equation for the capillary pressure was found recently by Holcomb and Zollweg [20]. At small Eo their equation yields (cf. Eq. (5))

$$y = 1 - 0.6689 Eo .$$

In most experiments with MBP-method $Eo \ll 1 (y \cong 1)$, i.e., the gravitational effect in Eq. (2) is negligible. For example, in our experiment Eo varies between 3.8×10^{-4} for pure water ($\sigma = 72$ dyn/cm) to 7.9×10^{-4} for micellar solutions of SDS ($\sigma = 35$ dyn/cm). Subsequently, the dynamic surface tension is calculated in all cases by means of Eqs. (1) and (2). The accuracy in measuring the surface tension is better than 0.2 dyn/cm.

Dead-time correction

There are two stages of formation of a bubble on the tip of a capillary [3]. During the first stage the bubble grows until the maximum pressure ΔP_{max} is reached and a hemispherical form is established. At that time $\sigma(t)$ corresponds to the surface tension of an air/water interface, aged for time t. Afterwards the bubble expands spontaneously during the second stage. The pressure inside then drops and the bubble leaves the capillary. The duration of the second stage is termed dead time, t_d. Hence, to determine the net time of the surface age, we should use the formula

$$t = t_v - t_d ,$$

where $t_v = \nu^{-1}$ is total time, measured experimentally.

To derive an expression for t_d, Feinerman [7] has considered Poiseulle flow of the air in the capillary. In this way he has obtained the approximate formula

$$t_d = \frac{32\mu_\alpha L_c}{R_c \Delta P} \left[\frac{\sigma}{R_c \Delta P} \left(\frac{R_b}{R_c} \right)^2 + \frac{1}{3} \left(\frac{R_b}{R_c} \right)^3 \right] \quad (8)$$

valid at $R_b \gg R_c$. Here μ_α is the air viscosity; L_c is the capillary length; R_b is the radius of the bubble during the stage of spontaneous expansion. Equation (8) shows that t_d may depend on the geometrical parameters of the capillary and on the surfactant concentration through σ. Garrett and Ward [12] have experimentally proved this statement by using an electronic counter, an oscilloscope, and a high-speed cinecamera. They have established that t_d does not depend manifestly on ν. In their experiment t_d is around 19 ms for distilled water and t_d is around 25 ms for SDS solution with concentration $\bar{c} = 7 \times 10^{-6}$ mol/cm^3. Their capillary has a radius 10^{-2} cm. Since L_c and R_b are unknown in our experiment, we had to perform direct measurements of t_d.

To do so, we visualized (as in [5, 12, 21]) the pulsations of the pressure when bubbles are blown away. We replaced the water manometer, which is too inert for this purpose, with a sensitive pressure transducer. The signal from the transducer is amplified and depicted on the oscilloscope screen. The signal has a saw-like form, corresponding to the changes in the pressure. Hence, t is the time interval, which ΔP needs to reach its maximum value P_{max}, while t_d is the time interval, during which ΔP drops down to its initial value. In this way the bubbling frequency was measured from the screen with an accuracy 0.1 s^{-1}.

We measured t_d at different ν for distilled water and several SDS solutions. We found that the dead time does not depend notably on the bubbling frequency (t_d varied between 15 and 25 ms). The results are plotted in Fig. 2. It is seen that with increasing the frequency the contribution of t_d increases in comparison with total time $t_v = \nu^{-1}$. The data for t_d are too scattered, because the dead time was measured with an accuracy of 5 ms, due to the low dividing ability of the oscilloscope screen. That is why the dependence of t_d on the concentration, predicted by Eq. (8), cannot be observed. The linear fit of the experimental data in Fig. 2 is $t/t_v = 0.99217 - 0.01824\nu$. Hence, the dead time is given by

$$t_d = 18.24 + 7.83/\nu , \quad (9)$$

where ν is in s^{-1} and t_d is in milliseconds. Equation (9) differs from the empirical formula of Austin et al. [2]

$$t_d = 39.9 - 0.252\nu . \quad (10)$$

Equation (10) is obtained for a capillary having different radius ($R_c = 5 \times 10^{-3}$ cm) and probably different length L_c. Both Eqs. (9) and (10) are compared in Fig. 2.

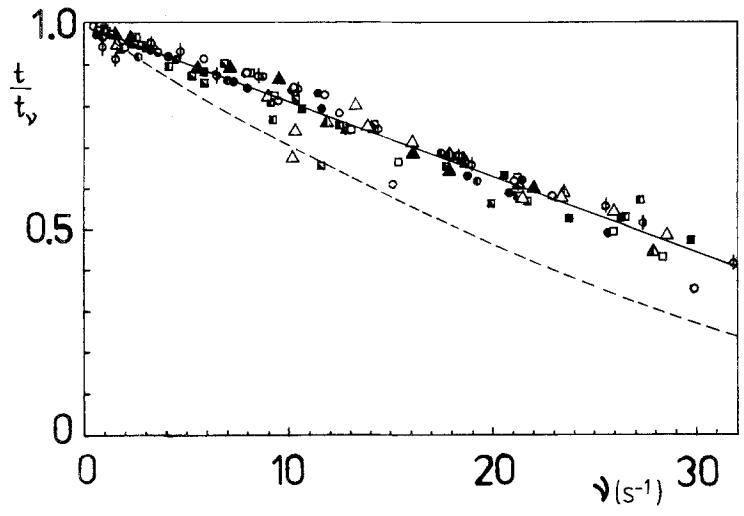

Fig. 2. Frequency dependence of t/t_ν for SDS solutions with different concentration (mol/cm^3): 0(○), 2×10^{-6}(○), 3×10^{-6}(●), 4×10^{-6}(□), 6×10^{-6}(■), 7×10^{-6}(△), 8×10^{-6}(△), 1.2×10^{-5}(◁), 1.6×10^{-5}(▶), 2.4×10^{-5}(×), 3.2×10^{-5}(+). The solid line is a linear least square fit by Eq. (9). The dashed line corresponds to Eq. (10)

Results and discussion

In Figs. 3 and 4 are given the experimental data for the dynamic surface tension of SDS and Veranol H10 solutions as a function of the bubbling frequency. It is seen that our data for SDS are in a good agreement with the MBP-data of other authors [11, 12], plotted also in Fig. 3 for concentrations equal or very close to the concentrations used by us. In Figs. 5 and 6 are given the respective plots of the dynamic surface tension of the two surfactants vs time t. For all concentrations the dead time corrections are performed by means of Eq. (9).

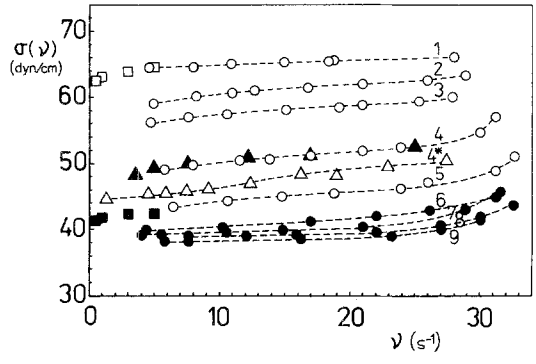

Fig. 3. Experimental dependence of the dynamic surface tension σ on the bubbling frequency ν at different SDS concentrations (mol/cm^3): 2×10^{-6} – curve 1; 3×10^{-6} – 2; 4×10^{-6} – 3; 6×10^{-6} – 4; 8×10^{-6} –5; 1.2×10^{-5} – 6; 1.6×10^{-5} – 7; 2.4×10^{-5} – 8; 3.2×10^{-5} – 9. The open circles (○) represent the data below CMC, and the filled circles (●) are those above CMC. The data of Garrett and Ward [12] are: 5×10^{-6}(△) and 7×10^{-6}(△) – curve 4*. The data of Woolfrey et al. [11] are: 2×10^{-6}(□) and 8×10^{-6}(■)

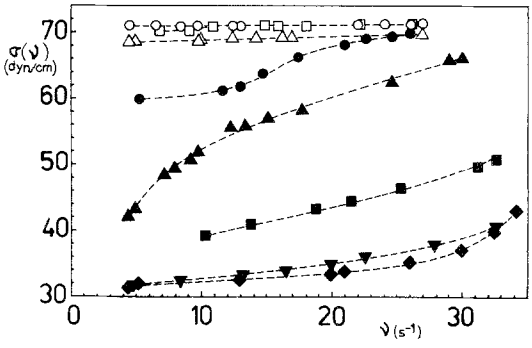

Fig. 4. Experimental dependence of the dynamic surface tension σ on the bubbling frequency ν at different Veranol H10 concentrations (mol/cm^3): 3.16×10^{-9}(○); 10^{-8}(□); 3.16×10^{-6}(△); 10^{-7}(●); 10^{-6}(△); 3.16×10^{-5}(■); 10^{-5}(▽); 3.16×10^{-4}(▶)

With increasing the frequency ν, very short times become accessible. For such short time intervals the bubble surface remains almost clean, because the surfactant molecules do not have time to adsorb onto it. Therefore, in this case the surface tension tends to the value of pure water. In the opposite case (low frequencies ν, i.e., large t) the surfactant molecules have enough time to reach the bubble surface and to adsorb onto it. In this way they sufficiently lower the surface tension.

It is seen from Fig. 5 that at infinite times the surface tension of SDS tends to its equilibrium values (the bars on the righthand side frame of the figure). (The equilibrium values are calculated by means of Eq. (11).) The SDS monomers are transported in short time (of the order of milliseconds)

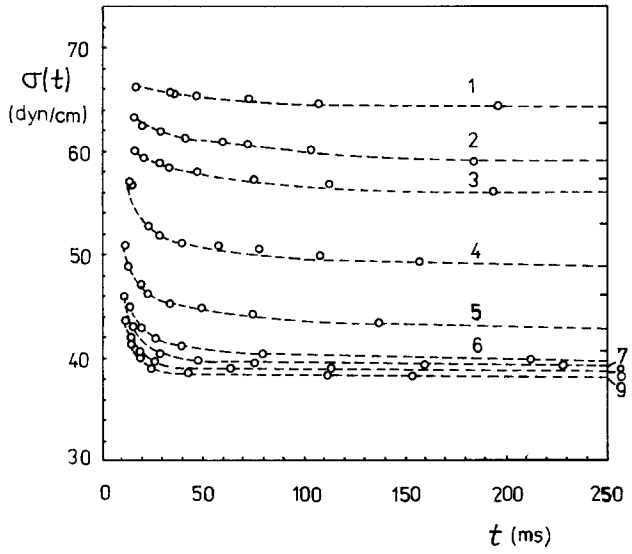

Fig. 5. The time dependence of the surface tension σ of the SDS solutions obtained by the data in Fig. 3. The bars denote the respective equilibrium values $\bar{\sigma}$ calculated by Eq. (11)

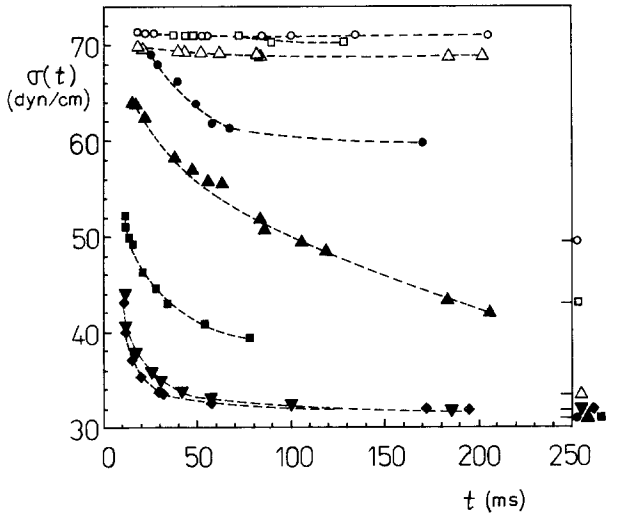

Fig. 6. The time dependence of the surface tension σ of the Veranol H10 solutions obtained by the data in Fig. 4. The bars denote the respective equilibrium values $\bar{\sigma}$

to the surface to produce a rapid relaxation of the surface tension. In the time interval covered by the experiment the surface tension of Veranol H10 below CMC is very far from its equilibrium values. (The equilibrium values of σ [13], denoted by the signs for the respective concentrations, are shown on the righthand side of Fig. 6.) This means that the characteristic time of transportation of Veranol H10 monomers is much greater than the respective time for SDS.

Figures 7 and 8 represent the dependence of the dynamic surface tension on the surfactant concentration of SDS and Veranol H10 at two different times. The equilibrium surface tension of SDS (Fig. 7) is calculated using the equation of Mysels [22]

$$\bar{\sigma} = 68.49 - 6.516\ln\bar{c} - 3.353\ln^2\bar{c}\,. \qquad (11)$$

Here $\bar{\sigma}$ is in dyn/cm, while $\bar{c}$ is in mmol/l. Equation

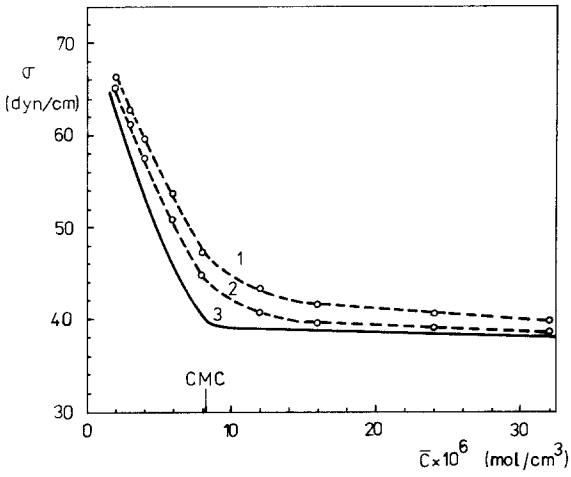

Fig. 7. The concentration dependence of the dynamic surface tension of SDS solutions at 10 ms (curve 1) and 50 ms (curve 2) obtained from the data in Fig. 5. The equilibrium curve 3 is drawn by Eq. (11)

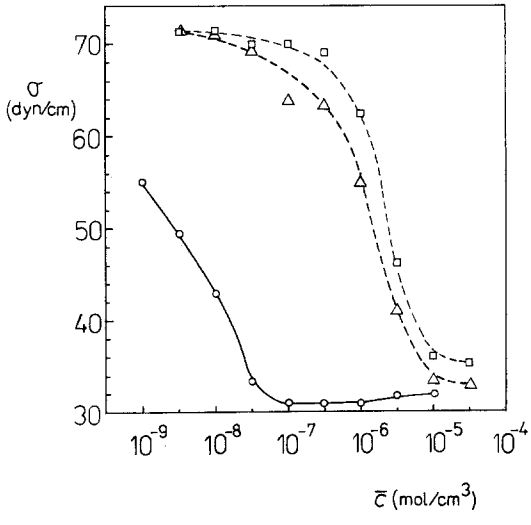

Fig. 8. The concentration dependence of the dynamic surface tension of Veranol H10 solutions at 20 ms (□) and 50 ms (△) obtained from the data in Fig. 6. The equilibrium data are (○)

(11) was obtained in [22] by fitting experimental data, obtained by the Wilhelmy plate method. The CMC of SDS is supposed to be 8.3×10^{-5} mol/cm^3.

The equilibrium surface tension data of Veranol H10 are taken from [13]. It is seen from Fig. 8 that $\bar{\sigma}(\bar{c})$ exhibits a minimum around CMC (CMC is accepted to be 5×10^{-8} mol/cm^3). The best fit of the data below CMC is

$$\bar{\sigma} = 54.96 - 3.705 \ln \bar{c} - 0.727 \ln^2 \bar{c} \,, \qquad (12)$$

where $\bar{c}$ is in μmol/l. Figure 8 illustrates the very large difference between the dynamic surface tension and the equilibrium surface tension of Veranol H10 in comparison with the respective curves of SDS in Fig. 7. This fact, due to the weaker transport ability, is also observed for other surfactants in [4, 23].

If the surfactant concentration increases, the relaxation of the surface tension becomes much faster (see Figs. 5 and 6). As we see, below CMC this may be attributed to the accumulation of surfactant monomers in the bulk of solution. The transport of material to the surface becomes more intensive and the surface equilibrates rapidly. To describe this process more quantitatively, we will use the equation for the monomer concentration in the subsurface layer $\Phi(t)$ derived in the subsequent paper [14]:

$$\Phi(t) = \bar{c}_1 \{1 - E[(t/\tau_D)^{1/2}]\} \,. \qquad (13)$$

Here, $\bar{c}_1$ is the equilibrium monomer concentration and $E(z) = \exp(z^2)\operatorname{erfc}(z)$ where $\operatorname{erfc}(z)$ is the error function complement. The characteristic diffusion time τ_D represents the ability of the surfactant molecules to enhance the relaxation. The subsurface concentration Φ can be obtained experimentally from the data of σ. Fitting these data by Eq. (13), we found that the values of τ_D for SDS range from 5.8 to 15 ms [14]. Of the same order are also the values of τ_D obtained experimentally by Garrett and Ward [12]. For Veranol H10 a sufficiently larger value of τ_D, 14.7 s was computed at concentration $\bar{c} = 3.16 \times 10^{-18}$ mol/cm^3 [15]. With increasing the surfactant concentration τ_D generally decreases. Hence, Eq. (13) predicts that the surface tension relaxation will really become faster.

In addition, above CMC the number of the free monomers remains almost constant: the excess amount of surfactant added transforms into micelles. In non-equilibrium conditions the micelles can disintegrate into monomers and additionally supply the bubble surface with surface active material. Two relaxation processes of micellization are observed experimentally by the usual chemical relaxation methods like p-jump method [24]. The first process, called fast process, is attributed to the release of several monomers by a micelle in order to make it less stable. During the second process, which is called slow process, the micelles destroy to reach their equilibrium concentration. We will denote the time constant of this particular relaxation process by τ_M.

However, the micelles can also be transported towards the bubble surface. In such a way they can facilitate the adsorption, thus causing the surface tension to relax faster than in the case below CMC. Subsequently, the difference between the dynamic surface tension σ and the equilibrium one $\bar{\sigma}$, shown in Figs. 7 and 8, can be explained by the participation of the micelles in the mass transfer. If the transport of micelles and the micellization are much faster than the time intervals accessible in the experiment, the equilibrium surface tension should establish instantaneously. These processes should have comparable characteristic time in order that the effect of the micelles becomes observable. It is seen from Figs. 5 and 6 that the time intervals covered in our experiment are between 5 and 250 ms. The surface tension of SDS and Veranol H10 above CMC changes notably until 30–40 ms. Therefore, the characteristic time of micellization τ_M is to be in the millisecond range. Of the same order should be the characteristic time of transportation of the free monomers τ_D, too, because the last species act like mediators among the micelles and the surface adsorption layer.

In this case the subsurface concentration is given by another equation derived in [15]:

$$\Phi(t) = \bar{c}_1 \{1 - \exp(-t/\tau_D)\{b_1 E[(k_1 t/\tau_D)^{1/2} - b_2 E[(k_2 t/\tau_D)^{1/2}]\}\} \,, \qquad (14)$$

where $b_1 = (1 + G)/2$, $b_2 = (1 - G)/2$, $k_1 = (1 + G)^2/4$, $k_2 = (1 - G)^2/4$ and $G = (1 + 4\tau_D/\tau_M)^{1/2}$. Equation (14) predicts a faster relaxation than Eq. (13) depending on the ratio τ_D/τ_M. It is known from the experiments on the micellization kinetics [24] that τ_M usually decreases with increasing the surfactant concentration. This fact, together with Eq. (14) explains qualitatively why the

relaxation of the surface tension becomes faster for micellar solutions. The values of τ_M computed from the experimental data for $\sigma(t)$ of SDS are between 1.1 and 4.5 ms [15]. Of the same order are the values of the slow relaxation time measured by p-jump technique [24].

Acknowledgements

The authors thank Prof. Ivan B. Ivanov, Dr. Alex Nikolov, and Dr. Yordan Radkov for valuable discussions of the experimental results. The financial support of the Bulgarian Ministry of Science and Education is also gratefully acknowledged.

Appendix

Here, Eq. (2) is derived after [16]. The profile of the air bubble expanding on a capillary tip is given in Fig. 9. The origin of the coordinate system is placed on the bubble surface in such a way that the z-axis coincides with the capillary axis. Two forces act across the bubble surface: the force $\underline{F}$, accounting for both the pressure and buoyancy force, and the capillary force acting along the contact line. Hence, the force balance in z-direction gives

$$F = 2\pi R_c \sigma \sin\varphi \ . \tag{A.1}$$

Generally, the force F can be expressed as [25]

$$F = 2\pi \int_{-z_c}^{0} \Delta P B \dot{B} dz \ , \tag{A.2}$$

where $r = B(z)$ is the equation of the bubble profile ($\dot{B} = dB/dz$), while $\Delta P(z)$ is the pressure difference

$$\begin{aligned} \Delta P(z) &= P_\alpha(z) - P_w(z) \\ &= \Delta P(z_c) + \Delta\rho g(z - z_c) \ . \end{aligned} \tag{A.3}$$

By introducing Eq. (A.3) into (A.2) and carrying out the integration at $B(0) = 0$ and $B(z_c) = R_c$, one obtains

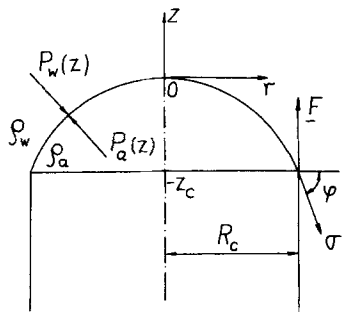

Fig. 9. Sketch of an air bubble expanding on a capillary tip (for notations see the text)

$$F = \pi \Delta P(z_c) + \Delta\rho g V \ , \tag{A.4}$$

where V is the current volume of the bubble

$$V = \pi \int_{-z_c}^{0} B^2 dz \ .$$

At the end of the first stage of the bubble growth the quantities become: $\varphi = \pi/2$, $V = 2\pi R_c^3/3$ and $\Delta P(z_c) = \Delta P_{max}$. Hence, combining Eqs. (A.1) and (A.4), Eq. (2) is obtained.

References

1. Kragh AM (1964) Trans Faraday Soc 60:225
2. Austin M, Bright BB, Simpson EA (1967) J Colloid Interf Sci 23:108
3. Bendure RL (1971) J Colloid Interf Sci 35:238
4. Huang DD, Nikolov A, Wasan DT (1986) Langmuir 2:672
5. Hua XY, Rosen MJ (1988) J Colloid Interf Sci 124:652
6. Kloubek J (1972) J Colloid Interf Sci 41:17
7. Feinerman VB (1979) Kolloidn Zh 41:111 (Russ)
8. Feinerman VB, Lylyk SV (1983) Zh Prikladn Chim 56:2218 (Russ)
9. Feinerman VB, Lylyk SV (1984) Kolloidn Zh 46:166 (Russ)
10. Miller TEJr, Meyer WC (1984) American Lab February:91
11. Woolfrey SG, Banzon GM, Groves MJ (1986) J Colloid Interf Sci 112:583
12. Garrett PR, Ward DR (1989) J Colloid Interf Sci 132:475
13. Radkov Y, Kralchevsky P, to be published
14. Dushkin CD, Iliev TzH, this journal, part 2
15. Dushkin CD, Iliev TzH, Radkov YS, this journal, part 3
16. Kralchevsky PA, unpublished results
17. Nayfeh AH (1973) Perturbation Methods. Wiley Interscience, New York
18. Johnson CHJ, Lane JA (1974) J Colloid Interf Sci 47:117
19. Sugden S (1922) J Chem Soc 121:858
20. Holcomb CD, Zollweg JA (1990) J Colloid Interf Sci 134:41
21. Mysels KJ (1982) Langmuir 5:442
22. Mysels KJ (1986) Langmuir 2:423
23. Petrova L, Radkov Y, Basheva E, Nikolov A (1986) In: Proc 6th Int Conf Surface Active Materials. Badstuer, DDR
24. Folger R, Hoffmann H, Ulbricht W (1974) Ber Bunsenges Phys Chem 78:986
25. Ivanov IB, Kralchevsky PA, Nikolov AD (1986) J Colloid Interf Sci 112:97

Received March 11, 1991;
accepted May 22, 1991

Authors' address:

Ceco D. Dushkin
Laboratory of Thermodynamics and Physico-chemical Hydrodynamics
Faculty of Chemistry
University of Sofia
1 Anton Ivanov Blvd.
1126 Sofia, Bulgaria